Available online at www.sciencedirect.com
ScienceDirect

Sensors and Actuators A 141 (2008) 34–42

SENSORS AND ACTUATORS A PHYSICAL

www.elsevier.com/locate/sna

Yield enhancement of piezoresistive pressure sensors for automotive applications

Marko Pavlin [a], Franc Novak [b,*]

[a] *HYB d.o.o., Trubatjeva 7, SI-8310 Sentjernej, Slovenia*
[b] *Jozef Stefan Institute, Jamova 39, Ljubljana, Slovenia*

Received 3 January 2007; received in revised form 13 June 2007; accepted 5 July 2007
Available online 22 July 2007

Abstract

An approach of enhancing yield in the production of piezoresistive pressure sensors for automotive applications is described. The main idea is to introduce an advanced pre-check, which sorts out potentially bad sensors before the actual calibration. The sorting algorithm is performed in two steps. In the first step, the linear correlation coefficient for the pre-checked sensor is calculated and compared to a margin initially estimated on the basis of the production first series and continuously adjusted during the mass production in accordance with the quality management strategy. In the second step, the actual values of coefficients of the pre-checked sensor are compared with the values of the reference coefficients. Both conditions must be met to enter the evaluated sensor in the calibration procedure. Empirical data from sensor production are given to illustrate the advantage of the described approach.

Keywords: Piezoresistive sensors; Calibration; Yield; Production test

1. Introduction

In manufacturing of modern electronic devices achieving and maintaining high yield level is a challenging task, which depends on the capability of identifying and correcting repetitive failure mechanisms. In most industries, yield has been defined as the number of products that can be sold divided by the number of products that can be made. The true yield number, however, is the number of functional and reliable products – shipped and paid for – minus the number of innocent bystanders (the perfectly good products rejected in the testing process) divided by the total manufactured [1]. Yield Enhancement defined as the process of improving the baseline yield for a given technology generation from R&D yield level to mature yield is one of the strategic topics of International Technology Roadmap for Semiconductors [2]. The concept is based on yield learning, which is a collection and application of knowledge of manufacturing process in order to improve device yield through the identification and resolution of systematic and random manufacturing events. Although primarily focused on semiconductor wafer technology the concept of yield improvement is general and can be applied to other electronic technologies.

Electronic sensors are massively involved in modern industrial automation applications. While sensor design and fabrication techniques including yield reports have been published in numerous papers, little publicity has been given in particular to the yield enhancement. One of the most time consuming steps in sensor production is calibration. Each sensor is individually exposed to several reference input signals and its transfer function is calibrated such that electrical output signal corresponds to the measured physical signal within the prescribed tolerance ranges. Significant loss in total production yield may result from the loss in calibration system. The calibration system has finite number of calibration places. Every sensor, which has failed after calibration represents missed opportunity to produce a good part and diminishes overall yield of the production process.

In this paper we describe the approach of enhancing yield in the production of piezoresistive pressure sensors for automotive applications. The main idea is to introduce an advanced calibration pre-check based on continuous learning from the calibration results of the past production. The process is schematically

* Corresponding author. Tel.: +386 1 4773 386; fax: +386 1 2519 385.
E-mail addresses: mp@hyb.si (M. Pavlin), franc.novak@ijs.si (F. Novak).

0924-4247/$ – see front matter © 2007 Elsevier B.V. All rights reserved.
doi:10.1016/j.sna.2007.07.017

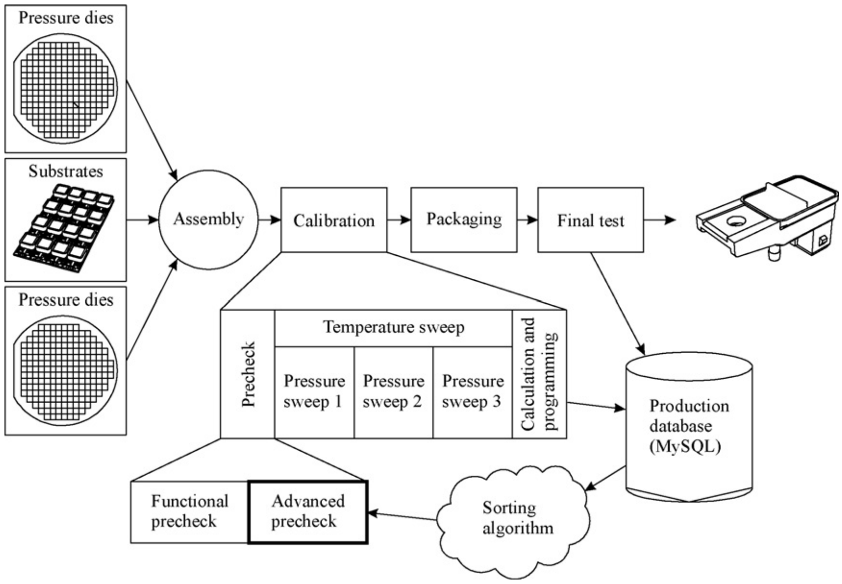

Fig. 1. MAP (manifold absolute pressure) sensor production.

depicted in Fig. 1 and will be described in more details in subsequent sections.

2. Automotive pressure sensor

A major obstacle in piezoresistive sensors compensation and calibration is the wide range of errors they exhibit. Primary error sources are [3]: strong, non-linear dependence of the full-scale signal on temperature (up to 1%/K), large initial offset (up to 100% of full scale or more at low pressure sensors), and strong drift of offset with temperature (packaging influence). In order to get the desired characteristic of the final product different algorithms and design strategies for calibration and temperature compensation are employed [4,5].

In our case, the pressure-sensing element is a silicon piezoresistive transducer shown in Fig. 2 and the calibration circuit is sketched in Fig. 3. The implanted piezoresistive structure forms a Wheatstone bridge. Provided in die form, the silicon dice is bonded on Pyrex socle. The complete measurement structure is mounted on a ceramic substrate. The sealed Pyrex socle allows using the sensor for absolute pressure measurement with vacuum as reference pressure. This type of pressure sensor consists of a micro-machined silicon diaphragm with diffused piezoresistive strain gauges.

The bridge resistance between Vcc and ground is constant over the operating pressure range. However, the bridge resistance changes with temperature at typically 800 ppm/°C rate. When the bridge excitation is constant-current source, the bridge voltage V_B is proportional to the bridge resistance. The bridge resistance change results in a bridge voltage change, which can be used as temperature signal for temperature compensation.

At given ambient temperature T and applied pressure p, the differential output voltage V_p is proportional to the bridge voltage V_B. Sensitivity S is sensor characteristics and is temperature dependant.

$$V_p = pS(T)V_B \tag{1}$$

The sensitivity S decreases with temperature due to the temperature dependence of piezoresistive coefficients in sensor's silicon structure.

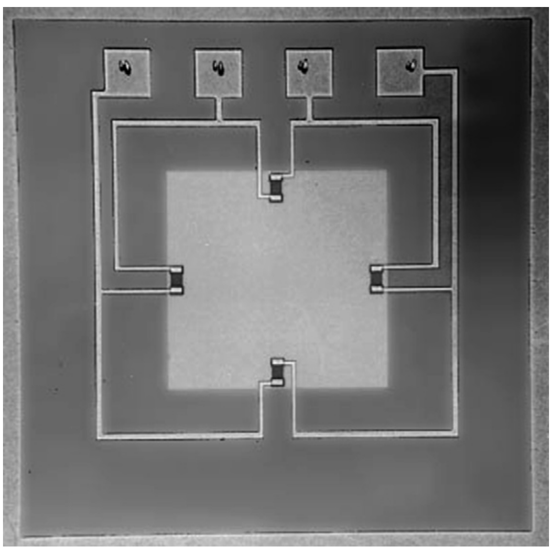

Fig. 2. Silicon piezoresistive transducer.

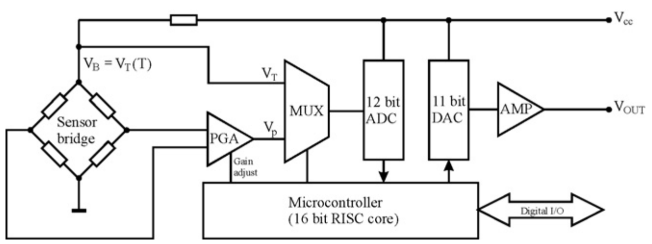

Fig. 3. Typical digitally calibrated pressure sensor.

The temperature compensation and calibration are done by two-chip digital sensor signal conditioner. Sensor bridge is piezoresistive silicon pressure sensor with vacuum as reference to measure absolute pressures.

As shown in Fig. 3, sensor bridge is connected to a digital sensor signal conditioner. The main task for the signal conditioning electronics is to correct errors induced in the sensing element by stimuli other than the primary sensing parameter. Magnitudes of errors vary from unit to unit, requiring calibration process in which each sensor is individually measured over the required operating range. Calibration is based on a numerical model, which can be defined by a multidimensional Taylor's series [6]. Calibration coefficients are represented by constants in Taylor's series. Based on the test data and calibration algorithm, the digital signal conditioning electronic circuit for each sensor is programmed with digital calibration coefficients stored in the internal calibration memory. Digital programming procedure minimizes sensor, interface, and electronics errors and makes external calibration components or laser trimming unnecessary.

In our case, a semi-custom ASIC is optimized for ratiometric differential sensors. Differential bridge signal is amplified with chopper-stabilized programmable gain amplifier, programmable to three differential gains (15.66, 24 and 42) and then converted with a single 12-bit input ADC. The 16-bit RISC microcontroller performs permanent correction calculation based on the pressure and temperature measurement. The corrected output signal is generated by a 11-bit output DAC. The temperature is sensed optionally through off-chip or on-chip diode. The correction processor has 16-bit ALU and (16×16 bit) RAM, ($1\text{k} \times 16$)-bit instruction ROM and (12×16)-bit parameter EEPROM. The correction formula is based on seven calibration coefficients stored in an EEPROM. The EEPROM stores the configuration word, calibration coefficients, upper and lower output signal limits and customer specific identifiers. Provided I2C interface serves for calibration purposes and the corrected sensor signal is also available as 12-bit digital word. The sensor signal conditioner implemented by ZMD31020 [8] is placed on a ceramic substrate together with silicon piezoresistive pressure die. To compensate sensor temperature errors, ZMD31020 is equipped by an external diode or by an on-chip pn-junction. Since the ceramic substrate provides high thermal conductivity and the pressure die is placed close to ZMD31020 both chips have the same temperature and internal pn-junction can be utilized [4].

The MAP (manifold absolute pressure) sensor, described in our case, is used for automotive applications. In particular, it takes part in the internal combustion engine's electronic control system. The manifold absolute pressure measurement is critical to an engine's electronic control unit (ECU) in order to calculate fuel and spark requirements. MAP sensor measures the "absolute pressure" (not manifold vacuum) in the engine's intake manifold. The mass of the air entering the engine is directly proportional to its density, which is directly proportional to the air's absolute pressure, and inversely proportional to the air's absolute temperature. Besides, MAP sensor can also be used to measure the barometric absolute pressure. [3]

3. Calibration algorithms

Numerous correction equations are available for sensor correction. The choice mostly depends on the behavior and nature of the uncorrected output of the sensor represented by the raw AD readout. The most appropriate compensation and calibration equation is based on the physics of the sensor element and its interfacing electronic circuit.

In general, sensor transfer function can be expressed by a multidimensional Taylor series [7,6]:

$$F(x_1, x_2, \ldots, x_n) = \sum_{i=0}^{D(1)}\sum_{j=0}^{D(2)}\cdots\sum_{p=0}^{D(n)} C_{i,j,\ldots,p}[x_1 - H_1]^i[x_2 - H_2]^j\cdots[x_n - H_n]^p \quad (2)$$

Typical pressure sensor compensation takes two parameters: digitized pressure voltage V_p from the pressure sensor element and digitized temperature feedback signal V_T (Fig. 3). The temperature signal is extracted from the pressure-sensing element or generated by a separate temperature sensor. Measured voltages are digitized and converted by using higher order, multisegment calculation of formula (2).

Silicon piezoresistive sensors have normally linear responses in the range below 0.1% FSO for pressure ranges around 1 bar and above. For automotive applications it is sufficient to use cubic polynomial approximation for pressure signal and linear function for temperature signal (3). The errors limiting final accuracy are in this case thermal hysteresis and sensor repeatability.

$$F(x_p, x_T) = \sum_{i=0}^{2}\sum_{j=0}^{1} C_{i,j}\left[x_p - H_i\right]^i\left[x_T - H_j\right]^j \quad (3)$$

Full operating range is divided into several segments by using piecewise polynomial segmentation.

Sensor signal conditioner has its calibration algorithm based on formula (3). The algorithm is optimized for the employed microcontroller. General form of sensor function is transferred to very specific formula, Eq. (4), based on raw, integer ADC readouts and scaled for minimal numerical errors and minimal required memory space for storing calibration coefficients [8,9]. Numerical operations are reduced to integer algebra within 16-bit precision.

$$F(x_p, x_T) = 2^{12}\frac{4x_p + 2^{-24}a_0x_p^2 + a_1 + 2^{-9}a_2x_T + 2^{-18}a_3x_T^2}{a_4 + 2^{-9}a_5x_T + 2^{-18}a_6x_T^2} \quad (4)$$

Eq. (4) is rewritten to form (3) in (5)

$$F(x_p, x_T) = \frac{C_0 + C_1x_p + C_2x_p^2 + C_3x_T + C_4x_T^2}{C_5x_T + C_6x_T^2} \quad (5)$$

Calculations are performed with minimal table size (number of polynomials) at maximal accuracy. There are other methods for approximation of sensor transfer function, like cubic splines [10]. The drawback of splines is larger number of multiplications

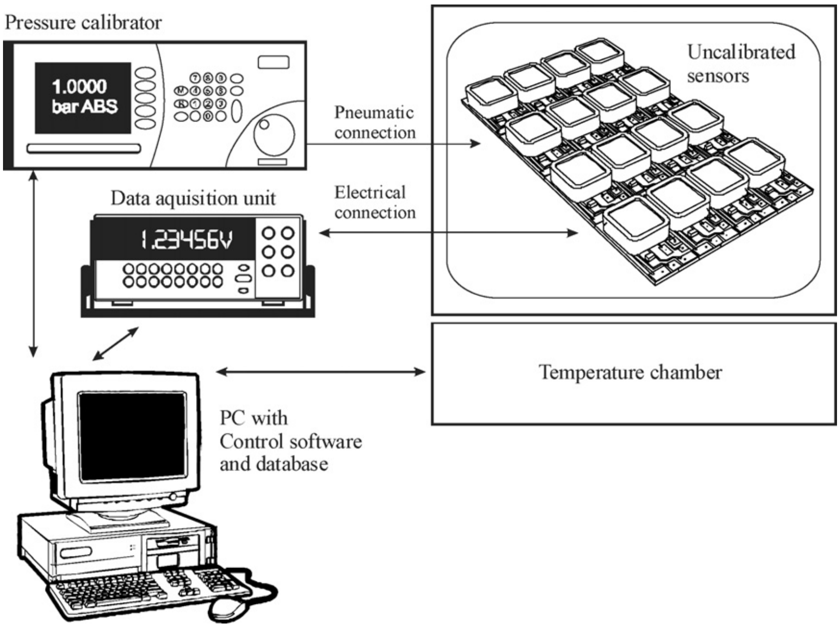

Fig. 4. Pressure sensor calibration equipment.

required for same output resulting in prolonged sensor signal delays and slower output signal update rate.

Transfer function approximation is adjusted to the target calibration range for each device. This is done by specifying the values of the calibration coefficients C_i stored in the DSSC internal non-volatile memory.

4. Calibration procedure

Calibration procedure is a process of determining coefficients in formula (5) by means of collected raw measurements from the pressure sensor bridge. The sequence of measurements is called *calibration scenario*. Each pressure sensor type has its own calibration scenario, which is defined in the product development phase. Scenario provides the shortest possible calibration time to obtain the required final accuracy for the specific sensor type.

Pressure sensors are calibrated in groups (128 sensors, in our case) at the same time. There is no general rule for determining the calibration lot size. It depends on calibration complexity, required production throughput and volume, calibration sensor type and requirements, etc. Normally, the calibration equipment is flexible to suit different requirements. Calibration system consists of a data acquisition station, temperature chamber and controlled pressure source. Readouts are acquired in sequence from each individual sensor. During this scanning process, the environment conditions must be stable to avoid measurement-induced errors in input vectors for calibration coefficient calculation. Elements of the calibration set-up are shown in Fig. 4.

Standard calibration scenario with three pressure points and three temperature points $\{3P/3T\}$ has 19 steps as shown in Table 1. Non-calibrated sensors are exposed to three different temperatures inside climatic chamber. During the first two steps, the calibration places are populated with assembled non-calibrated parts, hopefully without failures. The data for coefficient calculation is collected only after the whole scenario is completed (i.e., all sensors must be exposed to all temperature and pressure points).

If a failure is detected during calibration (for example, failures due to infant mortality, parametric failures, etc.), it is not possible to simply replace the failed sensor and continue with the scenario. Complete process has to be restarted from step 3 in Table 1. Consequently, replacement of bad sensors detected during calibration would cause enormous delays. It is therefore advisable to completely finish the running calibration even with some bad sensors. On the other hand, early detection of potential failures may have a significant impact on achieving high yield in mass production.

Table 1
Calibration steps for $\{3P/3T\}$ scenario

Step number	Operation	Time taken (min)
1	Set-up	2
2	Pre-check	2
3	T1 stabilization	15
4	P1 measurement	1
5	P2 measurement	1
6	P3 measurement	1
7	DAC calibration	3
8	T2 stabilization	15
9	P1 measurement	1
10	P2 measurement	1
11	P3 measurement	1
12	DAC calibration	3
13	T3 stabilization	15
14	P1 measurement	1
15	P2 measurement	1
16	P3 measurement	1
17	DAC calibration	3
18	Programming	1
19	Final test	4

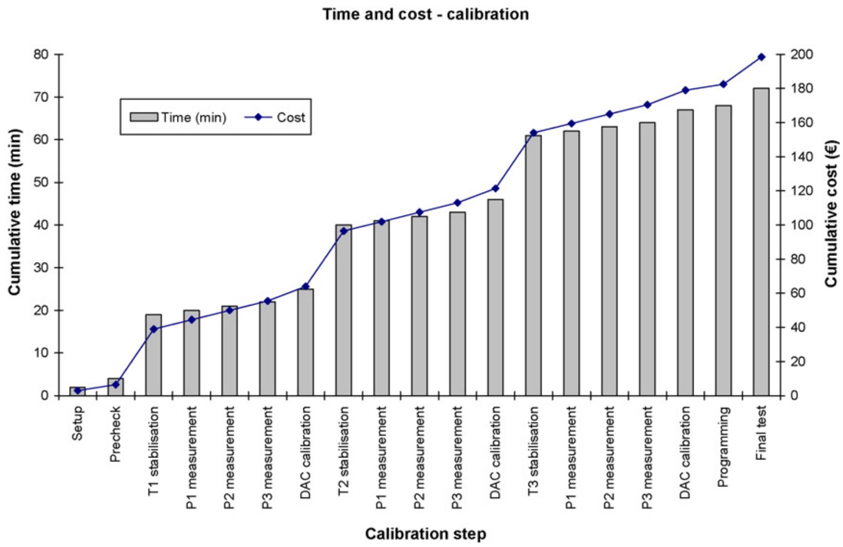

Fig. 5. Typical pressure sensor calibration timing.

Cumulative time and cost during calibration process for calibrating 128 sensors is shown in Fig. 5. Set-up and pre-check are finished quickly. The curve exhibits rapid rise after step 3. Every temperature stabilization step requires significant time interval. Complete calibration process is finished in about 70 min for typical $\{3P/3T\}$ calibration scenario. The presented scenario is just one of the possible calibration progressions. Other possible scenarios run at two pressure and temperature points. More than three measuring points on each axis are needed for higher targeted accuracy (Table 2). For standard industrial or automotive pressure sensors, scenario with three pressure points ($N_p = 3$) and two temperature points ($N_T = 3$) is sufficient for the accuracy 0.5%.

MAP sensor requires $\{3P/3T\}$ scenario in order to acquire data for solving the system of polynomial equations to derive coefficients $C_{p,t}$ from Eq. (5). Since pressure sweep is an order of magnitude faster than temperature sweep it is optimal to avoid multiple, unnecessary temperature transitions. Normally, temperature is set and after stabilization, pressure sweep is done to collect raw sensor responses (Table 1).

Before calibration, sensors are stored at room temperature. Since no temperature stabilization is allowed to keep any additional delays as short as possible, sensors are pre-checked at room temperature on docking working place. General sensor transfer function (3) is simplified to a single temperature point:

$$F(x_p, x_T) = \sum_{i=0}^{2} C_{i,0}[x_p - H_i]^i (x_T - H_0) \tag{6}$$

Table 2
Target accuracy of some other possible scenarios

Scenario	N_p	N_T	Typical target accuracy (%)
$\{2P/2T\}$	2	2	1
$\{3P/2T\}$	3	2	0.5
$\{3P/3T\}$	3	3	0.2
$\{4P/3T\}$	4	3	0.1

This simplified formula is the basis for sorting algorithms presented in this paper.

5. Calibration yield improvement

When pressure sensors are produced in high volume (automotive or medical applications), the manufacturing yield becomes a major economic factor. Not only achieved yield, but also the ability to rapidly achieve high yields is of crucial importance. High volume production of pressure sensors is usually based on a limited number of different types. While in most cases common circuit design, calibration algorithm and testing are employed there are, however, variations in housing and pressure range. Whenever a new sensor type is introduced, the yield drops at the beginning. A rapid yield ramp-up phase is required to catch the economic goals.

Normally, there are three distinctive sets of activities in the process of improving the yield: detection of yield loss, identification of the failure source (defect diagnosis) and corrective actions [11]. Due to the specific nature of pressure sensor production it is imperative to improve calibration yield since it has a direct consequence on the actual manufacturing yield. Calibration yield is the ratio between good parts after final test in calibration N_p and total number of calibration positions available N_0. It is assumed that calibration system is 100% occupied which is true for mass production.

$$\eta = \frac{N_p}{N_0} \tag{7}$$

Calibration yield can be improved by optimizing the number of sensors calibrated in a batch and by advanced pre-checking.

The balance between the number of parts in a batch and the cost of establishing conditions for such parallel process gives the optimal number of simultaneous calibrations. When the number of sensors calibrated in a batch is low, total production time for specific production volume may become prohibitively large. On the other hand, the cost and complexity of calibration

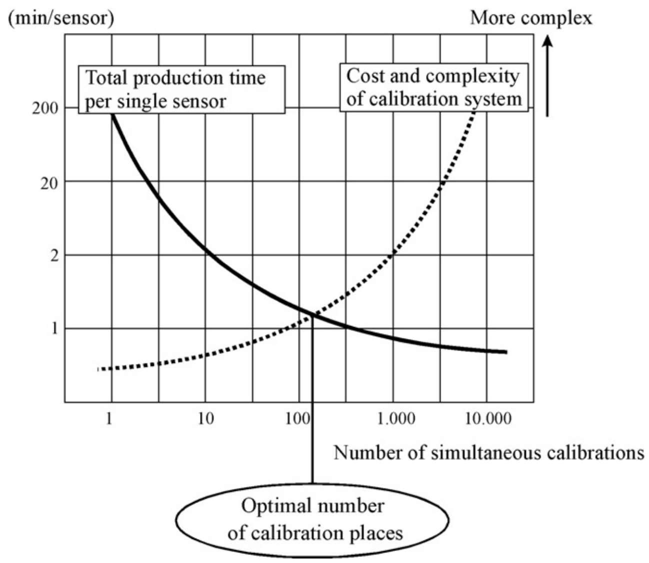

Fig. 6. Optimal number of sensors calibrated in a batch.

system grow with the number of sensors simultaneously processed (Fig. 6).

Conventional pre-check (step 2 in Table 1) sorts out only totally failed sensors. They are replaced with potentially good ones in the calibration system and the calibration procedure continues with step 3. Calibration is a time consuming task hence in order to be effective it should be performed on potentially good devices. Sensor bridges with large offsets or very small sensitivity cannot be calibrated. Calibration algorithm and its implementation in DSSC have limiting capability. Limitations come from different sources within the calibration electronic circuit (like saturation voltages) or limited precision resulted in numerical errors (e.g., integer division with small numbers). Every failed sensor occupying any of the 128 available calibration places increases yield loss. Identification of potentially bad sensors in the early pre-check phase is a prerequisite for calibration yield improvement.

The main challenge addressed in this paper is to find the set of pre-check parameters to sort out potentially bad sensors, which are out of calibration range. The objective is to find ranges for pre-check coefficients of expression (6) and their correlation to failures, which would distinguish possibly bad sensors from those which can be calibrated early in the pre-check phase two.

In such an advanced pre-checking, pre-check coefficients are calculated from the measurements performed at pressure sweep at room temperature. At the beginning of the sorting process, the limits are wide open allowing all sensors to pass the pre-check test. During early production stages for specific (or new) pressure sensor type these limits are continuously adjusted on the basis of correlation between the sensors failed after calibration and the values of pre-check coefficients. Ranges become more narrow and close to the optimal values. During the learning process it is possible to trim the sorting algorithm to be stricter and sort out even some sensors, which might be good at the end of calibration. The opposite direction of manual algorithm trimming results in relaxed margins allowing to pass even some bad sensors, which helps to avoid unnecessary loses on the expense of increased average calibration time. The line for sorting is not always sharp. Implemented algorithm presented in this paper allows flexible margins. An important feature is that it eliminates human errors due to wrong or subjective decisions.

6. Pre-check sorting background

Sorting algorithm is based on the measurements obtained at single, room temperature only. Consequently sensor characteristic (3) is simplified to

$$F(x_p, x_T) = \sum_{i=0}^{2} C_{p,0}[x_p - H_i]^i [x_T - H_0] \tag{8}$$

Measurements for pre-check are performed at N_p pressure points. Normal praxis is to measure at the offset pressure and at two different pressure points ($N_p = 2$), one close to the middle of the range and one near the full scale.

Assume that we have measured N_X sensors of the same type. Each sensor can be characterized at fixed room temperature with three coefficients from formula (8): C_{00}, C_{10} and C_{20}. Notice that the second index is 0 as the temperature is not changing and we are working at room temperature only. At specific time point in production the set of pre-check parameters is collected and used as a learning set table:

$$M_{\text{PC}} = \begin{pmatrix} C_{00,1} & C_{10,1} & C_{20,1} \\ C_{00,2} & C_{10,2} & C_{20,2} \\ \vdots & \vdots & \vdots \\ C_{00,N_X} & C_{10,N_X} & C_{20,N_X} \end{pmatrix} \tag{9}$$

First line in the learning set table M_{PC} describes characteristics at room temperature of the first measured sensor, next line, the second sensor from earlier production and so on. The above learning set will be used for pre-checking a new sensor with the following pre-check coefficients:

$$C_{\text{PC}X} = \{C_{00,N_X+1}, C_{10,N_X+1}, C_{20,N_X+1}\} \tag{10}$$

The sorting algorithm uses custom function $s(M_{\text{PC}})$, which calculates the probability of failure of each pre-checked sensor after calibration. Sorting function is specific for each sensor type and is based on the implementation of the corresponding calibration algorithm. Practical example is shown in the next section. Function $s(M_{\text{PC}})$ borrows some ideas from the algorithms reported in [12]. From theoretical point of view, optimal coefficient sorting algorithm for active feedback learning problems requires an exhaustive search of all possible subsets of pre-check coefficients of the chosen cardinality. For a large number of coefficients, this is may become quite impractical.

In our case, a limited set of coefficients allows us to simplify function $s(M_{\text{PC}})$ and to perform sorting algorithm within reasonable time limits.

Assume the finite number N_X of calibrated sensors with pre-check set of coefficients M_{PC} and the unknown sensor under evaluation with pre-check set of coefficients (10).

The sorting algorithm first calculates the reference set of sorting coefficients from the learning set (9) in the following way:

$$s(M_{\mathrm{PC}}) = \frac{1}{N_X}\left\{\sum_{i=1}^{N_X} C_{00,i} \sum_{i=1}^{N_X} C_{10,i} \cdots \sum_{i=1}^{N_X} C_{N_p0,i}\right\} \quad (11)$$

The result is the reference set C_{R} representing the mean value of all calibration coefficients.

$$C_{\mathrm{R}} = \{\overline{C_{00}} \quad \overline{C_{01}} \quad \overline{C_{02}}\} \quad (12)$$

Next, the linear correlation coefficient r (also called the product-moment correlation coefficient, or Pearson's r) between the unknown sensor coefficients C_{PCX} (10) and the average set C_{R} is calculated

$$r = \frac{\sum_{i=1}^{n}(x_i - \bar{X})(y_i - \bar{Y})}{\sqrt{\sum_{i=1}^{n}(x_i - \bar{X})^2}\sqrt{\sum_{i=1}^{n}(y_i - \bar{Y})^2}} \quad (13)$$

In the above expression, x_i are coefficients in $C_{\mathrm{PC}X}$ (10), y_i are the average reference coefficients in the set $s(M_{\mathrm{PC}})$ (12). Average values $\bar{X}$ and $\bar{Y}$of sets $C_{\mathrm{PC}X}$ and $s(M_{\mathrm{PC}})$, respectively, are calculated by

$$\bar{X} = \frac{1}{N_p}\sum_{i=1}^{N_p} C_{Xi,0}, \qquad \bar{Y} = \frac{1}{N_p}\frac{1}{N_X}\sum_{i=1}^{N_p}\sum_{j=1}^{N_X} C_{j0,i} \quad (14)$$

The linear correlation coefficient r has values in the range in the interval $[-1,1]$. Its value is close to one when the coefficients of the pre-checked sensor are in good correlation with the average reference coefficients.

The sorting algorithm is performed in two steps. In the first step, the linear correlation coefficient r for the pre-checked sensor is calculated and compared to a margin ρ_{PC}.

The value of ρ_{PC} is initially estimated on the basis of the production first series and continuously adjusted during the mass production in accordance with the quality management strategy. Depending on the type, production volume and sensor characteristics, adjustments can be performed manually or autonomously within the calibration software. If

$$r(C_{\mathrm{R}}, C_{\mathrm{PC}X}) > \rho_{\mathrm{PC}} \quad (15)$$

the sensor is passed to the second step otherwise it is replaced by a known good part. In the second step, the actual values of coefficients of the pre-checked sensor are compared with the values of the reference coefficients. Only the largest coefficient is compared with the corresponding reference coefficient

$$C_{\mathrm{PCMAX}} = \max(C_{\mathrm{R}}) \quad (16)$$

Assuming a predefined acceptance tolerance $\varepsilon_{\mathrm{PC}}$ the evaluated coefficient must lie within the interval

$$C_{\mathrm{PCMAX}}(1 - \varepsilon_{\mathrm{PC}}) > C_{Xi_{\mathrm{MAX}}0} > C_{\mathrm{PCMAX}}(1 + \varepsilon_{\mathrm{PC}}) \quad (17)$$

Both conditions (15) and (17) must be met to enter the evaluated sensor in the calibration procedure. Failed sensors are replaced with good parts and the calibration starts only by sensors that passed the pre-check procedure. For this purpose it is necessary to have some pool of good pre-checked sensors on stock. Some small additional time is needed when the failed sensors at pre-check are replaced in a single pass pre-check procedure as shown in Fig. 7.

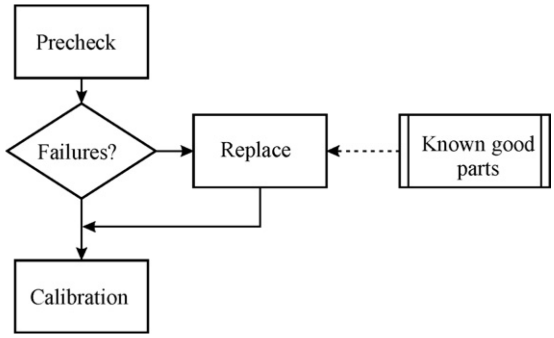

Fig. 7. Single pass pre-check procedure uses a pool of good pre-checked sensors to replace the failed parts.

7. Test results

The calibration phase in MAP sensor production (Fig. 1) employs modular calibration system consisting of several sensor calibrator modules shown in Fig. 8. A calibrator module provides interfacing to maximum 16 sensors. Each sensor is individually addressed and controlled by the instrumentation electronics. Interface provides the following control functions for each individual sensor being calibrated: power supply switching, I2C and single wire interface for each sensor, output voltage measurement with 16-bit precision and valve control for switching pressure or other actuators. The module is operated via RS-485 interface. Each module has its own 8-bit address, which allows up to 255 slave modules on same bus. Interconnection is done with four wires (two differential RS-485 lines and unregulated 12 V power supply). Sensor calibrator modules are connected to a single master module, with interfacing options to standard test equipment: ethernet with TCP/IP, USB or serial port. The data acquisition application is prepared in LabView.

When a new product is introduced, production database is created with no calibration data. Measurement results obtained

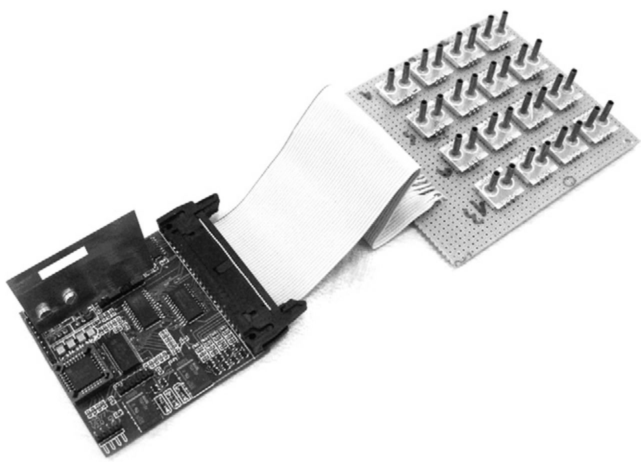

Fig. 8. Universal sensor calibrator with 16 pressure sensors.

Table 3
Statistical summary of learning set C_R ($N = 1034$)

	C_{00}	C_{01}	C_{02}
Mean	369.37	1870.61	1169.02
Standard error	2.10	3.21	2.53
Sample variance	4548.01	10622.37	6602.36
Range	550	708	632
Maximum	637	2217	1477
Minimum	87	1509	845

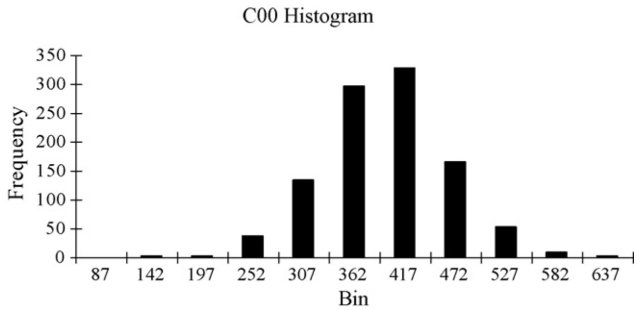

Fig. 9. Histogram for coefficient C_{00} from learning set ($N = 1034$).

from the good sensors in zero-series serve as the basis for the calculation of the initial learning set (9). In our case, the lot size of the zero-series was 1088 sensors resulting in 1034 good sensors after final calibration.

Some basic statistics relating the initial learning set are summarized in Table 3. Notice that the ranges of the initial values of coefficients are quite large due to a wide distribution of sensors' offsets. As the production quality improves, the deviation of parameters characterizing the product converges to a sharper distribution, which narrows the ranges of pre-check coefficients.

Histograms of learning set coefficients are given in Figs. 9–11.

As mentioned above, preliminary data collection was performed on total $N_A = 1088$ sensors from regular production. Functional pre-check (Fig. 1) revealed 11 faulty sensors before calibration step ($N_F = 11$). After calibration, 43 sensors did not pass the final test ($N_{FC} = 43$). Calibration yield for zero-series was

$$Y_A = 100\% - \frac{N_{FC}}{N_A - N_F} = 96\%$$

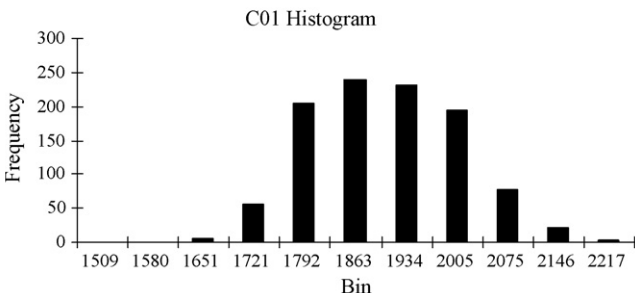

Fig. 10. Histogram for coefficient C_{01} from learning set ($N = 1034$).

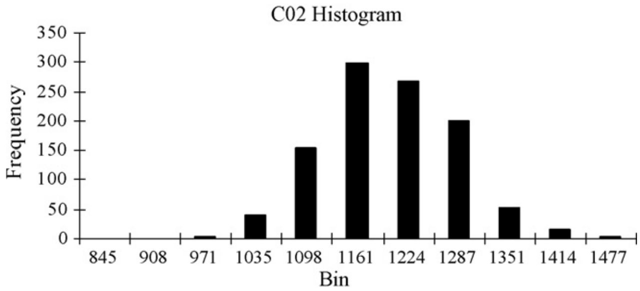

Fig. 11. Histogram for coefficient C_{02} from learning set ($N = 1034$).

The feasibility study indicated that 35 sensors out of 43 failed sensors would be detected if the advanced pre-check on the zero-series was employed. Hence, the total number of failed parts could be minimized to $N'_{FC} = 8$ and the calibration yield would increase to 99.2%.

$$Y_B = 100\% - \frac{N'_{FC}}{N_A - N_F} = 99.2\%$$

After initial promising results, the method was implemented in the production calibration software. By using the advanced pre-check in regular MAP sensor production the calibration yield is now maintained above 99%. Total number of produced sensors in the first series was $N_A = 13{,}832$. The number of failed sensors was 916, from which 793 sensors were sorted out by the advanced pre-check. With only functional pre-check the calibration yield would be only 93.4%. The actual yield as the result of successfully implemented advanced calibration pre-check was 99.1%. Subsequent series yield was further improved to 99.4% by the adjustments of sorting coefficients based on continuous learning.

Analyzing the total amount of time for calibration with and without the advanced pre-check, we assessed that 940 ms additional delay per sensor is spent for advanced pre-check when using 128 places for calibration. This time is negligible in comparison with the total calibration time (Table 1).

8. Conclusions

Manufacturing yield is an important issue because of its direct connection to profitability. Achieving yield close to 100% requires advanced and constantly improving techniques. Yield enhancement includes detection of failures and identification of defect sources in production process. Traditional approaches concentrate on sample based in-line inspection and the ability to diagnose faults and to correlate the results with possible sources of variation or defectivity.

In massive MAP sensor production, calibration scenario takes several minutes and its run-time optimization directly impacts production yield. Calibration yield can be improved by optimizing the number of sensors calibrated in a batch and by advanced pre-checking. The approach described in the paper employs fast pre-check based on a sorting algorithm with a margin continuously adjusted during production. Empirical production test data show that a significant yield improvement is achieved with little additional test time.

Acknowledgment

This work was partially supported by the Ministry of Higher Education, Science and Technology of the Republic of Slovenia under grant P2-0098.

References

[1] R. Madge, New test paradigms for yield and manufacturability, IEEE Des. Test Comput. 22 (3) (2005) 240–246.
[2] International Technology Roadmap for Semiconductors, http://www.itrs.net/home.html.
[3] S.M. Sze, Semiconductor Sensors, 1st ed., Wiley, New York, 1994, p. 550.
[4] J. Fraden, Handbook of Modern Sensors, Physics, Design and Applications, 3rd ed., Springer Verlag, 2004, p. 607.
[5] S. Soloman, Sensors Handbook, 1st ed., McGraw-Hill Professional, 1998, p. 816.
[6] IEEE Std. 1451.2, IEEE Standard for a Smart Transducer Interface for Sensors and Actuators—Transducer to Microprocessor Communication Protocols and Transducer Electronic Data Sheet (TEDS) Formats, The Institute of Electrical and Electronics Engineers Inc., 1998, ISBN 1-55937-963-4.
[7] D.C. Montgomery, Applied Statistics and Probability for Engineers, 3rd ed., Wiley, 2003, p. 720.
[8] ZMD31020, Differential Sensor Signal Conditioner Application, Note Rev. 1.3, July 25, 2002.
[9] J.W. Hauser, C.N. Purdy, Efficient function approximation for embedded and ASIC applications, in: Proceedings of the International Conference on Computer Design: VLSI in Computers & Processors, September 23–26, 2001, p. 507.
[10] K. Höllig, Finite Element Methods With B-Splines, Frontiers in Applied Mathematics, vol. 26, Society for Industrial and Applied Mathematics, 2003, p. 145.
[11] C. Hora, et al., An effective diagnosis method to support yield improvement, in: International Test Conference, Baltimore, USA, October 7–10, 2002, pp. 260–269.
[12] X. Shen, C. Zhai, Active feedback in ad hoc information retrieval, in: Proceedings of the 28th Annual International ACM SIGIR Conference on Research and Development in Information Retrieval, Salvador, Brazil, August 15–19, 2005, pp. 59–66.

Biographies

Marko Pavlin graduated from University of Ljubljana in 1995. Since 1995 he has been researcher at HYB Company in the industrial, medical and automotive sensor area. He was involved in development of new sensor devices and applications under several European Union projects. Currently he is working towards MSc degree in the field of pressure sensor production yield improvements. His main research interests include new medical sensor devices and wireless sensor networks for medical applications, wireless smart sensors, sensor production technology transfer to the third world and advanced production automation.

Franc Novak gained the BSc, MSc, and PhD degrees in electrical engineering from the University in Ljubljana in 1975, 1977, and 1988, respectively. Since 1975 he has been with the Jožef Stefan Institute, where he is currently head of Computer Systems Department. Since 2001 he is also assoc. prof. at Faculty of Electrical Engineering and Computer Science, University of Maribor. His research interests are in the areas of electronic testing and diagnosis, and fault-tolerant computing. His most recent assignment has been on design for testability of analogue circuits.